HAL
open science

Low Cost Flux Switching Linear Hybrid Actuator

Laurent Prevond, Jean Lucidarme, Bernard Multon

To cite this version:

Laurent Prevond, Jean Lucidarme, Bernard Multon. Low Cost Flux Switching Linear Hybrid Actuator. International Conference on Electrical Machines, Sep 1994, PARIS, France. pp.317-322. hal-00674062

HAL Id: hal-00674062

https://hal.science/hal-00674062v1

Submitted on 24 Feb 2012

HAL is a multi-disciplinary open access archive for the deposit and dissemination of scientific research documents, whether they are published or not. The documents may come from teaching and research institutions in France or abroad, or from public or private research centers.

L'archive ouverte pluridisciplinaire **HAL**, est destinée au dépôt et à la diffusion de documents scientifiques de niveau recherche, publiés ou non, émanant des établissements d'enseignement et de recherche français ou étrangers, des laboratoires publics ou privés.

ICEM'94 (Paris), 5-7 Sept. 1994, Vol.2, pp.317-322.

LOW COST FLUX SWITCHING LINEAR HYBRID ACTUATOR

ACTIONNEUR LINEAIRE HYBRIDE ECONOMIQUE A COMMUTATION DE FLUX

L.PREVOND, J.LUCIDARME , B.MULTON.
Laboratoire d'**E**lectricité **S**Ignaux et **R**obotique.
ENS CACHAN - URA CNRS D1375
61, av. Président Wilson
F 94235 CACHAN Cedex

Abstract

It's now possible to better satisfy the need for direct linear actuators. In particular, the household applications represent an expanding market. The principal constraints are the cost and the noise. We propose, in this paper, a new electromagnetic structure in which the rail is passive (without permanent magnets and without conductors) and where the mobile part (primary) has ferromagnetic pieces, permanent magnets and coils with simple forms very easy to build. The presence of permanent magnets permits obtaining good performances with high efficiency even for smaller sizes. Moreover the performances are not very sensitive to the air gap length in comparison with induction motors and switched reluctance motors. This last characteristic is important in order to have easy guiding. The present structure is cellular and works on the principle of permanent magnets flux switching during movement. We describe its principle, and we perform an analysis of the significant dimensional parametic influence. The electromagnetic phenomena is basically 3-D, but to simplify the understanding, the analysis is based initially on, an analytic modelling in linear mode, and then on a numerical computation by 2-D finite-element method. We then show an experimental structure for which we compare the theoretical results and the measurements of static effort. We also provide a synthesis of the experimental results obtained with many types of permanent magnets and with several numbers of cells. Finally, we show the results of the dynamic operation when the actuator is supplied by an electronic inverter and self-driving system with indirect position sensors.

Keywords
- Linear Actuator.
- flux switching.
- Permanent Magnet.
- Modelling.

Nomenclature

τ : pole pitch.
e : Total mechanical air gap.
R1, R2, Ra : Reluctances.
Rb : Resistance of a coil.
Va, Vb : Equivalent magnetomotive forces of permanent magnets and of the coils.
e.m.f : electromotive force.
u : Coil voltage.
ud : Sensor voltage.
U : Supply voltage.
ψ : Flux linkage
Fd : Detent effort.
σ_T : air gap magnetic shear stress.
M_L : mass of the Load.
M_{act} : mass of the actuator primary.

Introduction

The linear movements needed are numerous and require specific actuators. The production of linear movement can be direct (hydraulic jack or electromagnetic linear actuators) or indirect (motors with screw/nut system or wheel and gear). The indirect transmission systems are mechanically complex ; they are sometimes irreversible, bulky or noisy and often have poor efficiency. The need for electric linear actuators has existed for a long time, and some applications appear notably in the field of conveyors, positioning tables for tooling machines and in railroad traction.

We can consider two families of electromagnetic linear actuators, those having a short course (electromagnet, voice-coils...[1]) and those with a long course (or even no limitation). The unlimited course actuators, like the induction, switched reluctance motors etc., must have a poly-phase primary and a rail with or without any permanent magnet or conductors. Note that the rail can be primary, too (active rail). This permits suppressing the problem of mobile primary supply, but the cost increases noticeably to minimise its price and its size, we chose to develop a passive rail (without coils and without permanent magnets). Three types of electromagnetic linear actuators can satisfy this constraint: the induction motors, switched reluctance motors and hybrid motors.

The asynchronous linear actuators have some very low performances for small dimensions and a poor power factor [6]. The switched reluctance linear actuators have some dependent air gap value performances which pose problems for small dimensions (for a centimetric pitch). The development of a small mechanic air gap over the entire rail length introduces significant important normal efforts and require a high-quality, and thereby expensive, guide. The hybrid actuators have many advantages, like the permanent magnetic polarisation, without field copper losses and a lower influence of the air gap value on the performances, so the guiding becomes cheaper. Otherwise, the permanent magnet cost, generally significant with respect to the total price, necessitates the use of a small quantity of high-performance permanent magnet or an arrangement of ferrite magnets which permits a high flux ("flux concentration"). Our proposed structure can use a large effective area of magnets.

The hybrid actuators permit a very large diversity of structures [1][3][4][7]. Among these all structures, we propose one with "flux switching"[4][5]. It allows obtaining a simple construction, a high "flux concentration", a large amplitude of field flux variation and, ultimately, a cheaper development cost. Its coil is centralised, with short turn ends ; it is very simple to make with an excellent filling factor.

I- Flux switching description

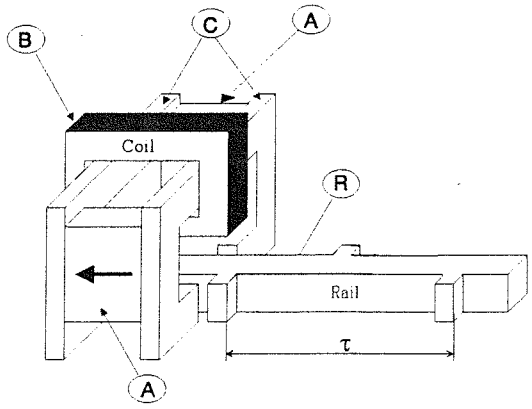

Figure 1 : Elementary Cell of the primary and the rail.

In this kind of flux switching electromagnetic machine with permanent magnet, the magnets and the coils are placed on the same ferromagnetic part, called primary. This is this part that moves along the rail. This primary movement on a toothed ferromagnetic-rail inverts the flux linkage. On one pitch, a large amplitude of alternative flux variation is obtained. This variation is larger than those we can obtain with magnetic polarised switched reluctance structures.

Figure 1 shows the elementary cell which works on this principle. The primary is made of permanent magnets (A) between two C-form ferromagnetic parts, a centralised coil (B) surrounding the two C and the permanent magnets. The rail (R) magnetically short-cuts one end of each C. The flux switching is made by the relative movement of the passive rail with respect to the primary. Effectively, the magnetic flux (shown by the dashed line in Figure 2a and 2b) alternates in the coil for the two shown specific positions. The centralised coil surrounds the two magnetic circuits (C), and so is thrown by an alternative flux, created by the permanent magnets and commuted by the passive rail.

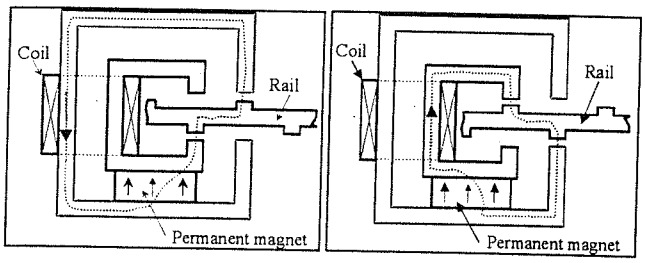

Figures 2a et 2b : .Planar elementary cell representation.

Furthermore, this configuration facilitates the juxtaposition of many cells while maintaining the overall coil wrapping (Figure 3), and the permanent magnets can occupy the entire area between the two C.

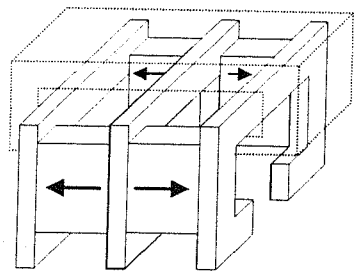

Figure 3 : Two elementary cells in association (with centralised coil).

To simply describe the functioning of this hybrid actuator, we propose an electric circuit-type modelling. Figure 4a shows a schematic representation of the elementary cell Figure 1. Because of symmetry reasons, the magnetomotive forces of the coil and of the permanent magnets are each separated in two generators, Vb and Va. Figure 4b shows the electromagnetic schema in which the reluctances R1 and R2 resemble the description in Figure 4c.

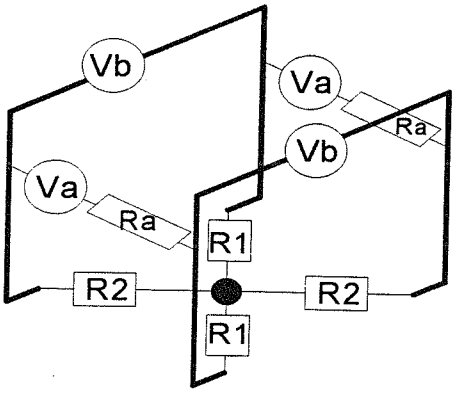

Figure 4a : Electric-circuit elementary cell
(the black central point represents the rail)

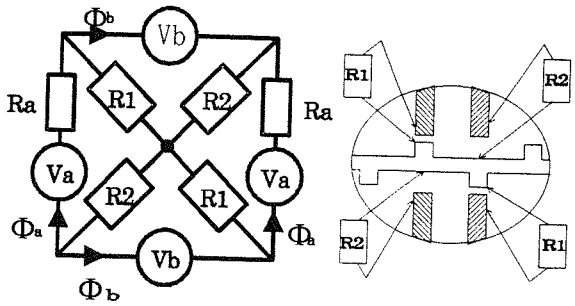

Figures 4b and c : Equivalent electric-circuit elementary cell.

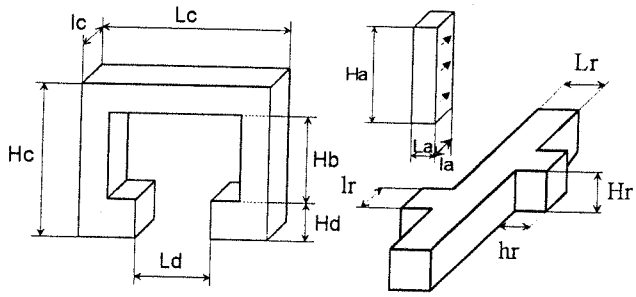

Figures 5 and 6 : Elementary cell piece dimensions.

Note that :

The mechanical air gap is : $e = Ld - Lr - 2.hr$

The pole pitch is : $\tau = 2.(lc + la)$

The cell length is : $Lcel = la + 2.lc$

Then :

With : R1, R2 the air gap reluctances which are functions of the position x.

$$Ra = \frac{1}{\mu_o \mu_a}\frac{la}{Sa} = \frac{1}{\mu_o \mu_a}\frac{la}{Ha.La}$$ is the permanent magnet reluctance.

$$Va = \frac{Br}{\mu_o}\frac{la}{\mu_a}$$: permanent magnet magnetomotive force with a remnance Br and a relative permeability μa.

$Vb = nI$: Coil magnetomotive force.
Φa : Half of total Permanent magnetic flux.
Φb : Half of coil flux.
F : instantaneous effort; <F> = mean effort for an ideal square current.

In the linear case (without saturation), we can write the following equations:

$$\begin{bmatrix} V_a \\ V_b \end{bmatrix} = \begin{bmatrix} R_a + R_1 + R_2 & R_2 - R_1 \\ R_2 - R_1 & R_1 + R_2 \end{bmatrix} \begin{bmatrix} \Phi_a \\ \Phi_b \end{bmatrix}$$

After the inversion of the matrix :

$$\begin{bmatrix} \Phi_a \\ \Phi_b \end{bmatrix} = \frac{1}{R_a.(R_1 + R_2) + 4.(R_1 R_2)} \begin{bmatrix} R_1 + R_2 & R_1 - R_2 \\ R_1 - R_2 & R_a + R_1 + R_2 \end{bmatrix} \begin{bmatrix} V_a \\ V_b \end{bmatrix}$$

This matrix form is :

$$\begin{bmatrix} \Phi_a \\ \Phi_b \end{bmatrix} = \begin{bmatrix} a & m \\ m & b \end{bmatrix} \begin{bmatrix} V_a \\ V_b \end{bmatrix}$$

With :

$$a = \frac{R_1 + R_2}{R_a.(R_1 + R_2) + 4.(R_1.R_2)} \; ; \; b = \frac{R_a + R_1 + R_2}{R_a.(R_1 + R_2) + 4.(R_1 R_2)}$$

$$m = \frac{R_1 - R_2}{R_a.(R_1 + R_2) + 4.(R_1.R_2)} \qquad (1)$$

The total magnetic coenergy is :

$$W'magn = \int_{0}^{Va} 2(m.V_b + a.V_a)dVa + \int_{0}^{Vb} 2(m.V_a + b.V_b).dVb$$

$$Vb=0 \qquad\qquad Va=cste$$

$$W'magn = a.V_a^2 + 2.m.V_a.V_b + b.V_b^2$$

The total effort can then be written as :

$$F = \frac{\partial W'magn}{\partial.x} = V_a^2.\frac{da}{dx} + V_b.\frac{db}{dx} + 2.V_a.V_b.\frac{dm}{dx} \qquad (2)$$

We clearly see in this formula three specific terms.

The first term corresponds to the effort due to the permanent magnetic magnetomotive force Va and to the reluctance variation and is called the detent effort.

The second one is proportional to the square of the current magnetomotive force, it is the reluctant effort.

The third is due to the interaction of the two magnetomotive forces of the permanent magnet and of the coil. This is the hybrid effort and is, in our structure the most important. Furthermore, we can notice that this is the only term that depends on the current sign. It is then possible to obtain a positive or negative effort along the entire pole pitch. We are reminded that this effort superposition is only valid in the linear case (no magnetic saturation).

With an ideal supply (a bi-directional current in the coil synchronised with the position), we obtain an instantaneous effort which is still positive on the entire pitch. We recall that the switched reluctance motors can give a positive effort on only half of the pole pitch.

Furthermore, note that the electromotive force has the same waveform as the hybrid effort, with (1) and (2) :

$$F_{hybrid} = 2Vb.Va.\frac{dm}{dx} \quad \text{and} \quad u = \left.\frac{d\phi b}{dt}\right]_{Vb=0} = Va.\frac{dm}{dx}.\frac{dx}{dt}$$

The basic and ideal supply consist of the injection of an alternative square wave current in phase with the e.m.f. (Figure 7a).

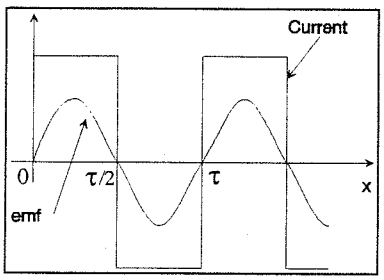

Figure 7a : Ideal supply.

We can use the induced voltage in the sensing coil to self-drive our actuator. This indirect self-driving sensor nonetheless requires a step-by-step start-up system because of the absence of e.m.f when the actuator is stopped.

II- Dynamic operation analysis.

The ideal supply provides an energy cycle area W corresponding to the converted energy of one phase on a pitch (Figure 7b):

$$W = 4\phi_{am} n\, Im$$

The average effort of a q-phased actuator is equal to :

$$< F >= q\frac{4.\phi_{am}.n\,Im}{\tau}$$

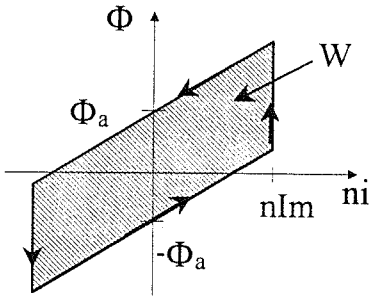

Figure 7b : Flux/ampere turns cycle.

The actuator's electromagnetic characteristics can be completely represented by the array of flux linkage characteristics of each phase with respect to the current and the position (Figures 7c and d) :

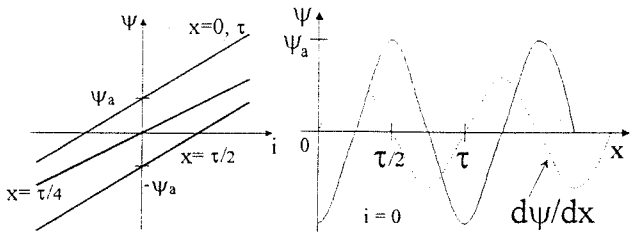

Figures 7c and d : Flux/ampere turns array and flux = f(x).

We have shown in Figure 7e the real flux/ampere turns of one phase of our fully-studied actuator (see chapter III-A).

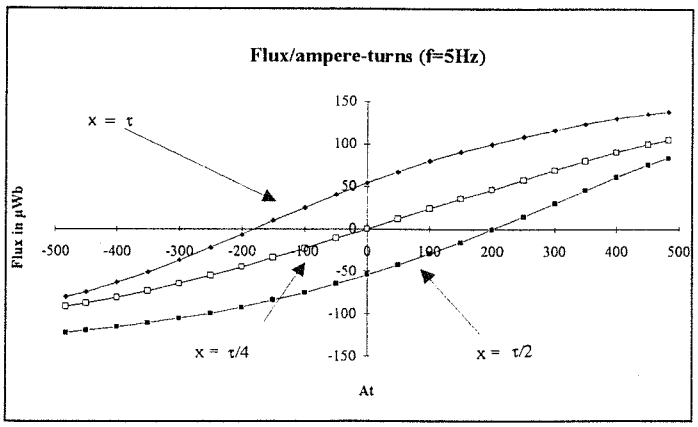

Figure 7e : Measured flux/ampere turns array.

These characteristics can be directly measured (Figure 7e) or reconstituted with static effort as a function of current and e.m.f. measurements. The equations which characterise the dynamic operations of the actuator, constituted by q mechanically tagged phases of τ/q+kτ and with a voltage supply (the coil resistance Rb naturally limits the current) are :

$$\pm U = R_b i_1 + \frac{d\psi_1}{dx}.\frac{dx}{dt}$$

$$\sum_{k=1}^{q}\left[\left.\frac{\partial W'_{em}}{\partial x}\right|_{i_1=cste} - Fd_k\right] = (M_{act} + M_L)\frac{d^2x}{dt^2} + F_L(x, \frac{dx}{dt})$$

where $W'_{em_k} = \int_0^{i_k} \psi_k . di_k$ is the coenergy of the phase k and F_{dk} is the detent effort of the phase k.

M_{act} is the mass of the actuator and M_L is the load mass.
We can note that in this kind of massive magnetic circuit, the magnetic losses reduce the useful effort when the frequency exceeds several dozen Hertz.

III- Modelling and simulation

A. Analogous Modelling

With the equations (1) and (2), we can draw the total effort wave form in the first harmonic approximation case for the R1 and R2 air gap reluctance variations (R1min. and R1max are analytically calculated [9]).

The presently studied case is for our actuator's elementary cell (Hd=10mm; lc=3mm ; Hc=30mm ; 2 ferrite permanent magnets, la=6mm La = 7.7mm ; Ha = 30mm):
Ra = 20,7 E6 H^{-1}
Va = 1670 A (Permanent Magnet ferram ARELEC Br=0.35T, μa = 1,04)
Vb = 500 A

R1 = 42,5 E6 + 32,5 E6 sin (2.PI*x/τ)

R2 = 42,5 E6 + 32,5 E6 cos (2.PI*x/τ)

In Figure 8, we can see that the detent and reluctant efforts have double the frequency of the hybrid and total efforts. Their average value is nul on one full pitch, but these efforts are resistant during one half-pitch and motor during the other half. The total effort is consequently "deformed".

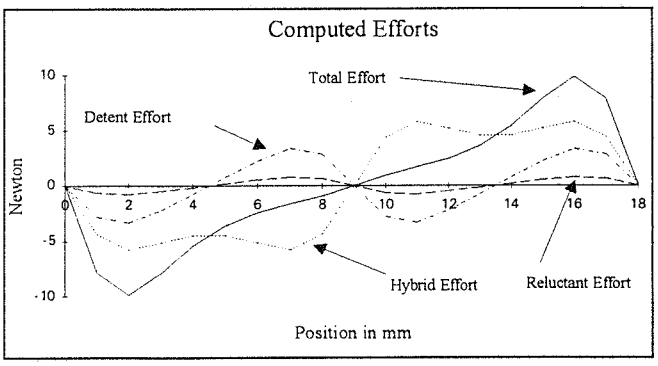

Figure 8 : Calculated effort form (Vb 500A).

The air gap magnetic shear stress σ_T is :

$$\sigma_T = \frac{<F>}{Su} \qquad \text{For one cell : } Su = 2.(Hd.Lcel)$$

We have calculated the variation law of the air gap magnetic shear stress versus the air gap length for one elementary studied cell and for 500A (Figure 9). We can see that, for example, if the mechanical air gap changes from 0.5 to 1mm, the effort is only divided by 1.5. This is a fundamental result (confirmed by the measurements, see tableau 1) for a linear actuator requiring an inexpensive, long-distance guide.

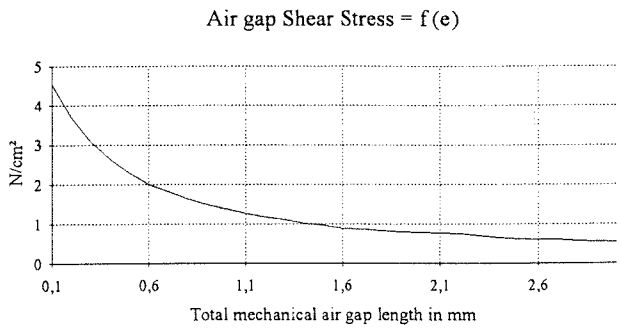

Figure 9 : σ_T as a function of the air gap.

This analytic modelling is very easy to use and needs only a weak computational power ; however, it supposes knowledge of the R1 and R2 reluctance forms if we are seeking a strong effort form. This method yields some good average effort results. This analytic modelling can provide a fast global optimisation of the structure if we can determine the R1 and R2 reluctance expressions as a function of dimensional parameters. To improve on the previous analytical results, we have used a finite-element numeric computation with a magneto static software 2-D (Maxwell 2-D). Initially, we calculate over the linear range (iron relative permeability of 1,000 corresponding to the massive soft iron used in our actuator).

B. Numerical Modelling.

Figure 10 shows the geometric model used in the 2-D finite-element computation. With this type of tool, we obtained on a pitch the effort forms, and we have defined the tooth-related dimensions of the rail permitting regular movement.

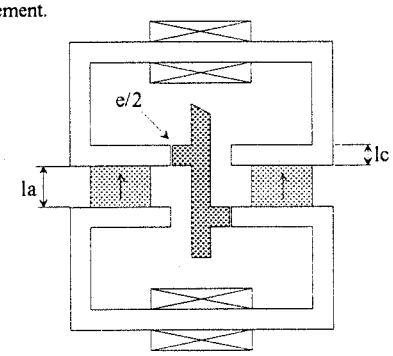

Figure 10 : 2-D model used in finite-element computation.

The computation conditions are :
μr = 1000 ; nI = 500 At ; Br = 0.35 T

The Figures 11a and 11b show the hybrid effort of one elementary cell of the studied actuator with a current of 500A for two tooth-widths lr of the rail (lr = 3mm with e=0.4mm, and lr = 5mm with e=0.8mm : lc = 3mm).

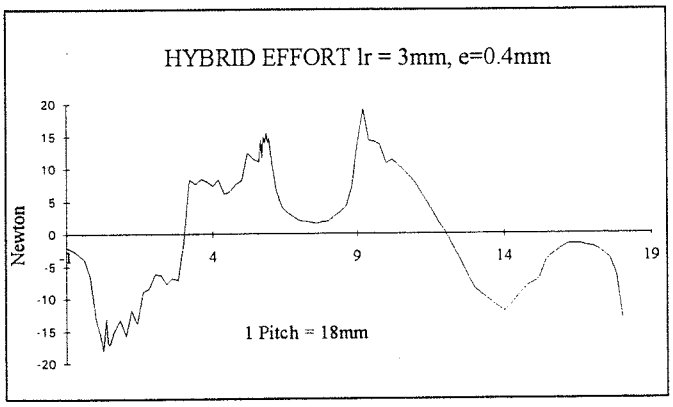

Figure 11a : Hybrid effort for e = 0.4mm and lr = 3mm.

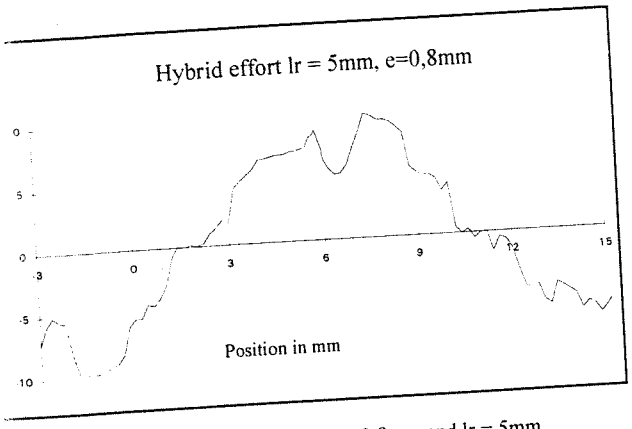

Figure 11b : Hybrid effort for e=0.8mm and lr = 5mm.

e form of the hybrid effort with the 5 mm-tooth width is better than with e 3mm, and the average value is higher relative to the air gap length. The crease of the air gap value (0.4 to 0.8mm) divides the maximal effort lue by around two. This numerical modelling allows making a geometric timisation of the structure, but this method is long and requires powerful mputation means and doesn't take into account 3D effects.

igures 13 and 14 compare the measured effort with those calculated by he analytical modelling and by 2-D finite elements.

IV. Experimental results.

Description of the studied actuator:

studied actuator is diphased, the total mobile part size (primary) is 100) x 60 mm. Each phase is composed of three elementary cells (four C 3 "groups" of two ferrite magnets La = 6 mm; la = 7.7mm ;Ha=30mm).

e rail is mounted on a rigid support which yields an efficient guiding. he useful rail tooth height is 10 mm (Hd=Hr). The lateral guidance is erformed by rollers to control the mechanical air gap on the entire rail ength.

The all-magnetic circuit (rail and C) is made of massive soft iron A37. This prototype is modulable : it is possible to put only one phase or only one elementary cell for specific testing. The actuator coils are made to accept 500At continuously. The resistance of each coil of 1000 turns is 35 Ohm at 20°C.
The actuator converter is made of integrated standard circuits which have two complete bridges of 1A peak under 40V. This integration is important for putting the electronic controls command on the motor.
The self-driving system is developed from one measure coil on each phase which give the position from the induced voltage (ud = e.m.f + ldi/dt).

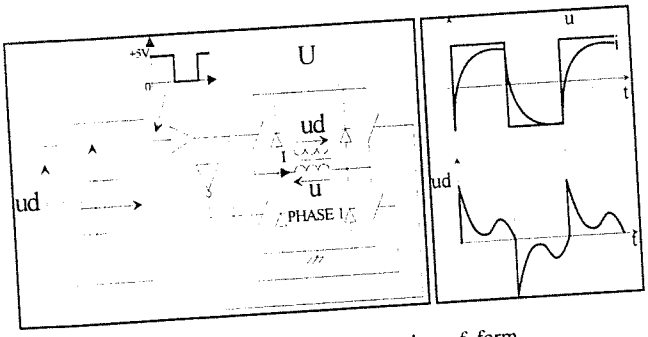

Figure 12 : supply schema and e.m.f. form.

The actuator start-up must be conducted step by step with few steps, and just after the self-driving system takes over. This start-up phase and all the operational security measures (end course security and untimely blockage) are conducted with a simple, cheap microcontroler. The entire power and command system are on the actuator, and so only two wires or two sliding contacts are necessary to supply the actuator.

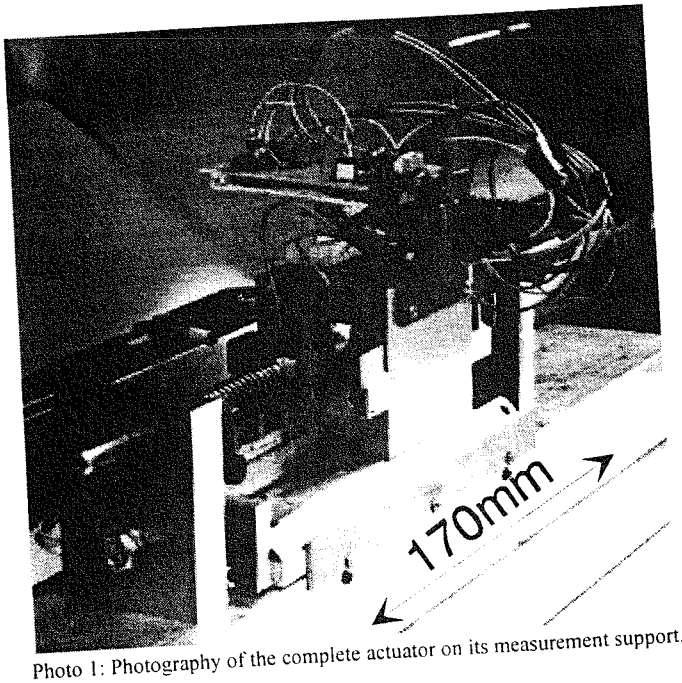

Photo 1: Photography of the complete actuator on its measurement support.

B. Experimental results and comparison with the model.

To qualify a linear actuator from a dynamic and static perspective, a specific test apparatus is necessary. Therefore, we have developed different tools for measuring the static form and value efforts, the speed and the e.m.f. We used an effort sensor, a position sensor and a micrometry system to position statically the actuator.

Static tests.

We present here in the measurement of the total effort of an elementary cell that we compared with the two models, analytical (see previous chapter III-A data , R1 and R2 are sinusoidal) and numeric.

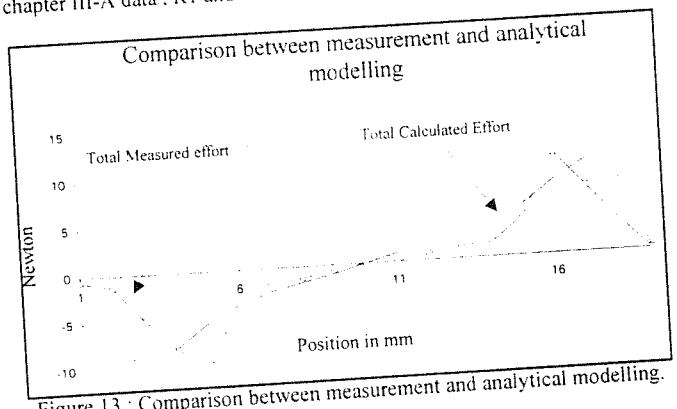

Figure 13 : Comparison between measurement and analytical modelling.

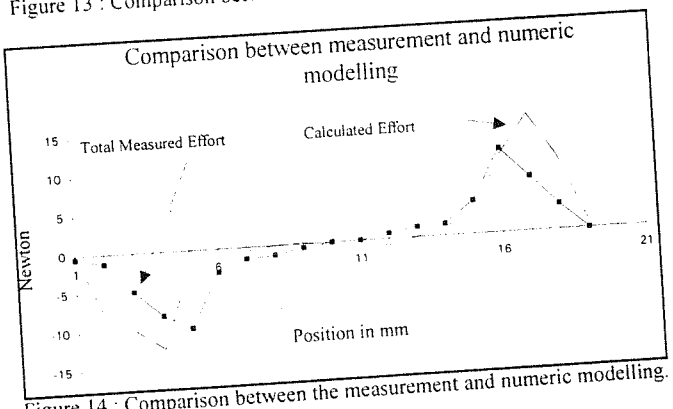

Figure 14 : Comparison between the measurement and numeric modelling.

The analytical and numeric modelling show a small displacement of the maximum effort. It seems to be due to the magnetic saturation that we haven't taken into account in our study. The measured values are different from the computation too because of the 3-D effect not taken into account. The tableau 1 resume the static results for many actuator configurations and for two permanent magnet types.

Thickness of the C (lc)	1.5mm	3mm								4mm
Permanent Magnet type	Ferrite	Ferrite								Fe Nd B with plastic
P.Magnet Thickness (la) in mm	2	2	6							5
Number of C	3	3	2		3	2x4	2x4	2x4		2
Rail tooth width (lr) in mm	1.5	3	5	6	6	3	5	6		5
Total mechanical air gap (e) in mm	0.4	0.4	0.45	0.4	0.4	0.35	0.45	0.4	0.8	0.4
nI=0 => Fd max. in N	1.3	1.2	2	2	3	4	4	5	1.2	10
nI=300At : <F> (N) σ_T (N/cm²)	1.8 1.4	2.5 0.96	1.5 0.7							
nI=500At: <F> (N) σ_T (N/cm²)		3.3 1.25	2.4 1	3.15 1.3	3.7 0.87	10.4 0.87	11.5 0.96	11.2 0.94	9.7 0.81	5.3 2
nI=600At: <F> (N) σ_T (N/cm²)	2.2 1.7	3.7 1.4	2.6 1.1							6.4 2.4
nI=1000At: <F> σ_T (N/cm²)			3.3 1.36			13 1.1	15.6 1.3	15.5 1.3	13.6 1.1	
nI=1560At: <F> σ_T (N/cm²)										9.7 3.7

Tableau 1 : static recapitulative measurement.

Principal remarks on the static measures :
The magnetic shear stress values of 1 N/cm² with ferrite permanent magnet are most satisfactory and with allied permanent magnet NdFeBo (Brémag 10 ARELEC Br = 0.65T), the value of 3,7 N/cm² is very satisfactory for this size of actuator. The influence of the mechanical air gap does not degrade too heavily the mean effort.
The assemblage of two elementary cells shows the saturation effect of the central ferromagnetic part. Figure 15 shows the real form of the diphased static effort for the ferrite actuator supplied with 500At.

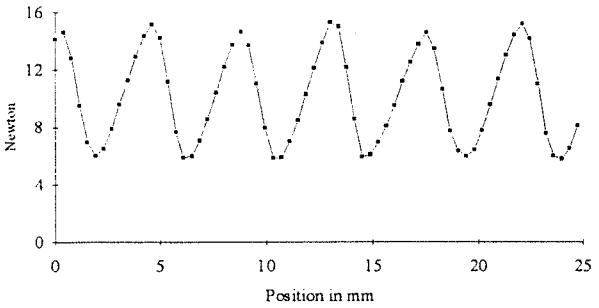

Figure 15 : Total static effort of the diphased actuator (lr = 5mm).

Dynamic Tests
We show in Figure 16 a curve of the movement as a function of the time and the supply voltage with a constant load (10N) in the indirect sensor for the self driving case.

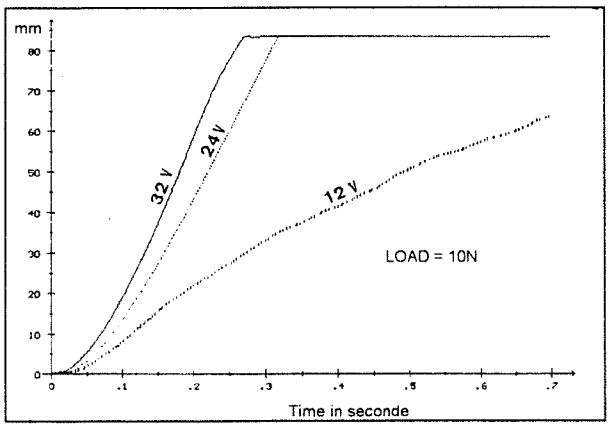

Figure 16 : Dynamic operations with self-driving system.

Figure 16 shows position as a function of time with the actuator supplied by several voltage values U (12V, 24V and 32V). The load effort is constant and equal to 10N, the load mass is 1kg. The speed is 0,24m/s with 24V.

Conclusions and perspectives

The structure of the actuator is new, very simple, cellular and very easy to build. The results obtained with this first unoptimised actuator are most satisfactory. The phenomena are fundamentally 3-D, but we have defined an analytical and a 2-D numerical model in the linear case. We have tested several actuator configurations (cell numbers, permanent magnet types, size parameters.....). Without saturation, the measured average effort is near the computed one, but the form is a little different because of the local saturation. To have a more efficient model, the saturation case must be studied, and the 3-dimensional finite-element study seems necessary.
Actually our effort pertains to the optimisation of the supply and the structure to improve the static and dynamic effort wave form in taking into account the magnetic losses.

References

[1] JUFER: Traité d'électricité, Dunod 1979
[2] H. YAMADA, Y. YAMAMOTO, H. WAKIWAKA, 'Linear pulse motor for implantable artificial heart', ICEM 88 (vol. II), 1988, pp.123-126.
[3] M. KANT. Les actionneurs électriques pas à pas. Hermés 1989.
[4] S.A. NASAR, I. BOLDEA, L.E. UNNEWEHR, 'Permanent Magnet, Reluctance, and self-synchronous motors', CRC Press, 1993(USA).
[5] G.A.J. AMARATUNGA, P.P ACARNLEY, P.G. McLAREN, 'Optimum Magnetic Circuit Configurations for Permanent Magnet Aerospace Generators', IEEE Trans. on Aerospace and Electronic Sys. vol. AES-21, N°2 pp : 230-255, March1985
[6] M. KANT, R. BONNEFILLE, Moteur linéaire à induction, Technique de l'ingénieur D551, 03/1980.
[7] T. KENJO. Stepping motors and their microprocessors controls, Oxford Publications, 1984-1992.
[8] G. LACROUX, Les aimants permanents, Technique et documentation-Lavoisier, 1989.
[9] D.P. TORMEY, D.A. TORMEY, P.L. LEVIN, 'Minimum air gap-permeance data for the doubly-slotted pole structures common in variable-reluctance-motors', IEEE Conf.IAS, 1990, pp.196-200.